

## SMALL-SIGNAL GAIN AND NUMERICAL SIMULATION OF TRANSVERTRON HIGH POWER MICROWAVE SOURCES

Donald J. Sullivan, John E. Walsh\*, M. Joseph Arman, Brendan B. Godfrey

Mission Research Corporation  
1720 Randolph Road, SE.  
Albuquerque, New Mexico 87106-4245

The transvertron oscillator or amplifier is a new and efficient type of intense relativistic electron-beam-driven microwave radiation source. In the  $m = 0$  axisymmetric version, it consists of single or multiple cylindrical cavities driven at one of the  $TM_{0np}$  resonances by a high-voltage, low-impedance electron beam. There is no applied magnetic field and the oscillatory transverse motion acquired by the axially-injected electron beam is an essential part of the drive mechanism. The transvertron theory was systematically tested for a wide range of parameters. The simulations were designed to verify the theoretical predictions, assess the transvertron as a possible source of intense microwave radiation, and study its potential as a microwave amplifier. Numerical results agree well in all regards with the analytical theory. Simulations were carried out in two dimensions using CCUBE with the exception of radial loading cases, where the 3-D code SOS was required.

### Introduction

The  $m = 0$  transvertron is an unmagnetized annular electron beam driven cavity resonator. It is in effect a negative resistance oscillator which produces high levels of monochromatic radiation at frequencies near the  $TM_{0np}$  resonances of the cavity. Unlike the elementary monotron, the energy exchange process depends essentially on the oscillatory radial motion of the beam electrons and this leads to a number of interesting characteristics. Among these are the comparatively short cavity length required in order to start the oscillation and the high saturation level.

In a series of simulations the operating frequency, the small-signal gain, the saturation level, and the extraction efficiency have been examined. The initial investigation focused on the characteristics of a source operating in the 1-GHz range, although extrapolation to other frequencies is straightforward. In simulations which included an output coupling structure (several radial waveguides), extracted power levels exceeded several gigawatts at an rms efficiency of 30 percent. The results of the simulations are also found to compare favorably with the predictions of a simple analytic model of the device. We anticipate that an average or energy efficiency of 50 percent is realistically obtainable.

### Transvertron Theory

The general theory of transvertron sources has been presented elsewhere.<sup>1</sup> Here we will concentrate on the  $m = 0$ , unmagnetized version. Although the physics is similar for arbitrary cross-section cylindrical cavities, we will concentrate on right circular cylindrical geometries. A diagram of the source is shown in

\*Permanent address: Dartmouth College, Hanover, New Hampshire.

Fig. 1. It consists of a cylindrical cavity of length  $L$  and radius  $R$ . The injected beam is positioned near the cavity wall and has an annular cross-section. The beam is azimuthally symmetric and, hence, it couples most strongly to the TM modes of the structure. In practice, the  $L/R$  ratio is never much greater than unity, and the  $TM_{011}$  mode is dominant. Since there is no applied magnetic field at saturation, both radial and axial beam modulation play a role in the energy exchange process. The former contribution is dominant in the cases tested; because of this, the  $TM_{0n0}$  modes, which lack an  $E_r$  component, are not excited.

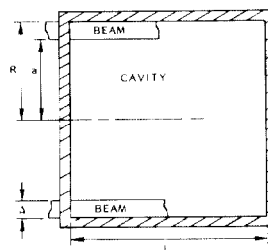


Figure 1. Transvertron schematic diagram showing the annular beam entering through the cavity surface on the left.

The energy exchange process can be understood in simple terms. The entering beam is unmodulated, and it is assumed that an individual beam electron follows an orbit determined by the electromagnetic fields present in the cavity at the time it enters. During an electron transit time the field amplitude change may be neglected and, hence, the energy exchange depends upon the amplitude of the field components and the relative phase at the time of entrance. The sign of the phase average net exchange of energy between the beam and the resonator fields will be a function of the transit angle,  $\Theta$ . This parameter is defined by  $\Theta \equiv \omega\tau$ , where  $\omega$  is the resonant frequency of the cavity and  $\tau$  is the average transit time of an entering electron. In the small-signal gain regime  $\tau$  is well approximated by the ratio  $L/v_0$ , where  $v_0$  is the initial electron velocity.

A quantitative expression for the relative rate of energy exchange may be obtained from the complex form of Poynting's theorem:

$$\frac{1}{Q_b} \equiv \text{Re} \frac{-1}{2\omega W} \int_{\text{beam}} \underline{J}^* \cdot \underline{E} \, dV \quad (1)$$

where  $\underline{J}$  is the modulated current induced on the beam by the fields,  $\underline{E}$  is the electric field, and  $W$  is the stored energy. The reciprocal quality factor  $1/Q_b$  generally will be an oscillatory function of  $\Theta$ . In regions where it is negative, the stored energy will grow exponentially in time.

When evaluated for the present geometry (TM<sub>011</sub> mode), the dominant terms in Eq. 1 yield the estimate

$$-\frac{1}{Q_b} \approx \frac{8I_b}{\beta\gamma I_0} \left[ \frac{J_1(2.405a/R)}{J_1(2.405)} \right]^2 \cdot \frac{L^2}{R^2} \cdot \frac{\pi^2(\Theta^2 - \pi^2/\beta^2)(1 + \cos \Theta)}{\Theta^3(\Theta^2 - \pi^2)^2} \quad (2)$$

Terms not yet identified are  $\beta$  and  $\gamma$ , the relative velocity and energy of a beam electron,  $I_b/I_0$ , the beam current in units of 17 kA, and  $a$ , the mean beam radius. The magnitude of the gain also depends on the square of the ratio of the  $J_1$  Bessel function evaluated at the beam's mean radius and at the wall.

When the cavity geometry is fixed, the value of  $\Theta$  for a given mode is determined and, thus, it is not the most convenient free parameter. A better choice is the ratio of the length and the radius. The resonant frequency for the TM<sub>011</sub> mode is

$$\omega = c\sqrt{\frac{\pi^2}{L^2} + \frac{2.405^2}{R^2}} \quad (3a)$$

which may also be expressed in terms of

$$\Theta = \frac{\pi\sqrt{1+x^2}}{\beta} \quad (3b)$$

where

$$x = \frac{2.405L}{\pi R} \quad (3c)$$

A plot of  $-1/Q_b(x)$  is shown in Fig. 2. Also shown on the figure are values of  $1/Q_b$  determined from a series of computer simulations.

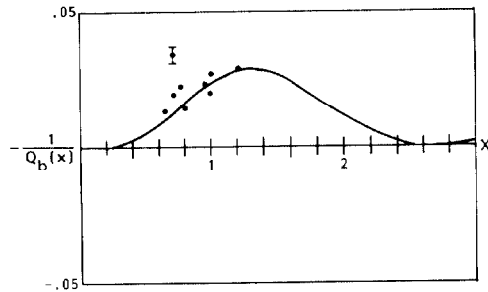


Figure 2. The function  $-1/Q_b(x)$  from Eq. 2 and the results of particle simulation runs where  $I_b = 35$  kA,  $V_b = 1.5$  MV and  $R = 35.5$  cm. The cavity length was varied and  $x$  was determined by Eq. 3. A typical uncertainty in the growth determination is displayed.

The parameters chosen for the comparison were a voltage,  $V_b = 1.5$  MV, a current  $I_b = 35$  kA, and  $R = 35.5$  cm. An error bar is indicated on the figure, and these represent the small uncertainty in the growth determination. The agreement is good. In general Eq. 2 is oscillatory, and growth of higher-order (TM<sub>01p</sub>) modes is possible. Some choices of the parameter  $x$  will result in fields

with the amplitudes of the higher harmonics nearly equal to the fundamental. Simulations performed with 750 kV and 4.0 MV beams and a variety of cavity dimensions show the same general characteristics and agreement with theory.

The formulation of the linear theory of the transvertron given above is complete, and the assumptions are consistent with conditions simulated. A nonlinear theory of comparable detail does not yet exist. However, with the aid of simple arguments, it is possible to determine the general nonlinear characteristics.

The dimensionless gain in the linear regime (Fig. 2) reaches zero at certain points along  $x$ , which in turn corresponds to a given transit angle, say  $\Theta_s$ . If the beam was injected with a velocity which placed it at  $\Theta_s$ , no energy would be exchanged with the fields in the cavity. Alternatively, if the beam is injected at some other value of  $\Theta$  (say,  $\Theta_0$ ) such that growth occurs, the field amplitude will reach a point where the assumption that the electron orbit is a straight line will no longer be valid. When the velocity modulation is large enough to carry a beam electron from  $\Theta_0$  to the vicinity of  $\Theta_s$ , wave growth would be expected to saturate. The value of  $\Theta_s$  determines a velocity  $\beta_s$  and an energy  $\gamma_s$ , which, with the aid of the equations of motion for a typical electron, finally determines a field amplitude at saturation.

The radial component of the field thus determined, when multiplied by the cavity radius and displayed in units of the beam voltage, is given by:

$$\frac{V_{rs}}{V_b} = \frac{\pi}{\beta_0(\gamma_0 - 1)} \cdot \frac{\gamma_0 - \gamma_s}{1 + \cos \Theta_s} \cdot \frac{x^2 + 1/\gamma_0^2}{x\sqrt{1+x^2}} \quad (4)$$

Once again, it is convenient to display Eq. 4 as a function of the relative length  $x$ .

The observed saturation amplitude for the same series of simulations whose growth rate is displayed in Fig. 2 is plotted in Fig. 3. A sharp variation with  $x$  is apparent. At the position

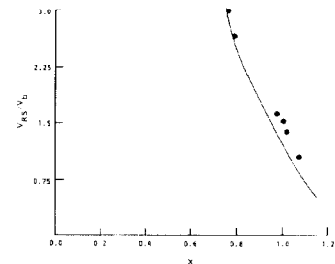


Figure 3. The observed saturation amplitude (dots) for the simulations shown on Fig. 2. The solid line is the prediction of Eq. 4, normalized to unity at  $x = 0.75$ .

$x = 0.75$ , Eq. 4 predicts a value of  $V_{rs}/V_b = 4.5$ , which is about 50 percent higher than the observed value. However, when the relative size of  $V_{rs}$  at this point is adjusted to give agreement with the simulation value, the observed trend is followed closely by the prediction given in Eq. 4. This is shown as a solid line in Fig. 3. In view of the approximate nature of the argument, the agreement is excellent.

## Transvertron Amplifier

In addition to the single-cavity system, we have also simulated a two-cavity system as the basis for an RF amplifier. An annular beam enters the first cavity from the left and interacts with the RF signal fed into the first cavity. After amplifying the signal, the beam enters the second cavity strongly bunched by the fields in the first cavity, resonates with the second cavity and radiates more energy before leaving the system. The  $TM_{011}$  modes of both cavities are, of course, matched to the frequency of the input RF signal. Input/output takes place through waveguides provided on both cavities. In the simulation presented here, the beam parameters are 1.5 MV and 18 kA and the RF frequency is 1.36 GHz. The system can be scaled to frequencies covering the range 1-20 GHz, although issues of RF vacuum breakdown must be addressed at the higher frequencies.

Figure 4(a) depicts the axial trajectories of electrons for one (code) time step ( $1.8 \times 10^{-11}$  sec) before the instability has saturated. Figure 4(b) is the corresponding radial trajectories and shows that the radial motion of the beam plays an important role in the energy exchange. Note that because of the azimuthal

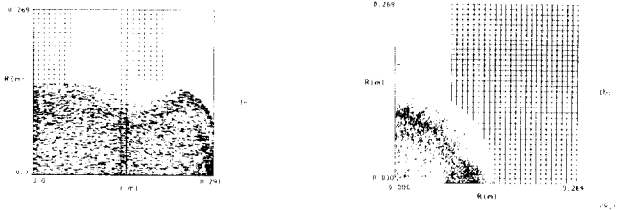


Figure 4. (a) Axial trajectories of beam electrons at  $t = 5$  ns showing their motion with respect to the cavities and the waveguides. (b) Radial trajectories of electrons at  $t = 5$  ns shown with the radial section of the first cavity and one of the waveguides.

symmetry in the geometry and in the mode selected, we have modelled only one quadrant of the full  $360^\circ$  azimuthal extent. Figure 5(a) is the particle plot of  $P_z/m_0$  (the electron's normal-

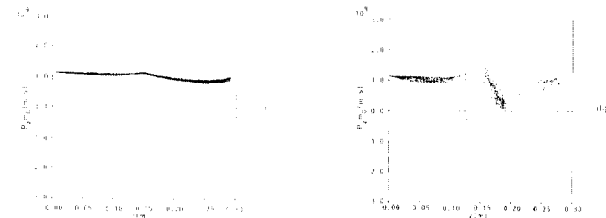


Figure 5. (a) Scatter plot of  $\gamma\nu_z$  vs.  $z$  before saturation showing a small space charge depression due to charges in the cavity. (b) Scatter plot of  $\gamma\nu_z$  vs.  $z$  after saturation, showing a reduction in beam momentum as it leaves the system.

ized axial momentum) as a function of the axial distance before the instability has grown appreciably. It reveals a slight space charge depression due to electrons in the cavity. Figure 5(b) is the corresponding particle plot after the instability has saturated and shows the beam momentum diminished as it leaves the system. A time history of the beam current in the second

cavity confirms strong bunching that exceeds 200% of the original 18 kA beam. Its Fourier transform indicates a pure  $TM_{011}$  frequency with at least six harmonics present due to the extreme current bunching, and no indication of any other modes in the cavity.

Figure 6(a) shows the initial input power (the first 20 ns) delivered to the first cavity, along with the power extracted from the first cavity through the input waveguides. The power extracted from the second cavity (not shown in Fig. 6(a)) is twice as large as that extracted from the first, because the saturated fields are larger in the second cavity. The gain based on the first cavity alone is larger than 20 db. The rms efficiency in this case is 18% for the two cavities. In a three-cavity amplifier, the rms efficiency reached 33%. With proper optimization, we believe efficiencies above 50% are possible. Figure 6(b) is the Fourier power spectrum of Fig. 6(a) showing a very monochromatic

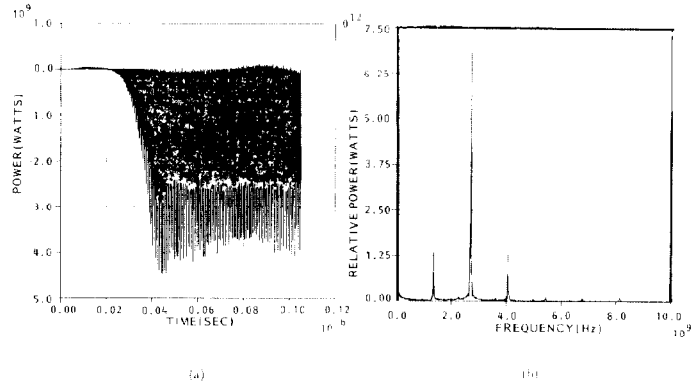


Figure 6. (a) The power extracted from the first cavity of the amplifier vs. time. The positive values between 0-20 ns indicate the input power fed through the same waveguides. (b) The Fourier transform of Fig. 6a showing a pure RF frequency for the extracted power with no other modes present.

oscillation at 1.36 GHz with some harmonics present. (Note: The Fourier transform of the power output is at twice the oscillation frequency). The total gain for the simulation presented here is 24 db. However, with a 10% increase in the saturation level obtained by changing the cavity  $L/R$  aspect ratio, the gain can be raised to 34 db. Without the input signal the amplifier produces no appreciable RF radiation in the cavities.

### Acknowledgement

This work was conducted for the Air Force Weapons Laboratory under contract F29601-86-C-0216. We would like to thank Mr. Robert Clark of MRC for his help in initializing the SOS simulations and his numerous discussions on the operation of the code.

### References

[1] B. B. Godfrey, D. J. Sullivan, M. J. Arman, T. C. Genoni, and J. E. Walsh, "Linear Theory of Transvertron Microwave Sources," submitted to SPIE's *OE/LAS'89*, 1988.